

Statistical properties of parameter-dependent classically chaotic quantum systems

Elizabeth J Austin and Michael Wilkinson

Department of Physics and Applied Physics, John Anderson Building, University of Strathclyde, Glasgow G4 0NG, UK

Received 22 October 1991, in final form 16 April 1992

Accepted by I C Percival

Abstract. In this paper we examine the dependence of the energy levels of a classically chaotic system on a parameter. We present numerical results which justify the use of a random matrix model for the statistical properties of this dependence. We illustrate the application of our model by calculating both the number of avoided crossings as a function of gap size and the distribution of curvatures of energy levels for a chaotic billiard: the distribution of large curvatures is determined by the density of avoided crossings.

Our results confirm that the matrix elements are Gaussian distributed in the semiclassical limit, but we characterize significant deviations from the Gaussian distribution at finite energies.

PACS numbers: 0365, 0545

1. Introduction

In many situations of physical interest it is important to understand how the energy levels of a system vary as a function of a parameter of the Hamiltonian: an important example is the dependence of the electronic energy levels of a molecule on coordinates describing the configuration of the nuclei. Figure 1 shows an example of the dependence of energy levels on a parameter for a system with chaotic classical motion: two important features of this plot are that it displays no apparent regularity, suggesting that a statistical description would be most appropriate, and that the curves do not cross, but occasionally approach each other at events called avoided crossings. In this paper we test a statistical model for the parametric dependence of energy levels, which is applicable to systems with a chaotic classical limit.

To build a theory describing the statistical properties of plots such as figure 1 we require statistical information about both the spectrum of the Hamiltonian $\hat{H}(X)$ for a fixed value of the parameter X , and the matrix elements of $d\hat{H}/dX$ in the basis formed by the eigenstates $|\phi_n(X)\rangle, |\phi_m(X)\rangle$ of $\hat{H}(X)$ (the adiabatic basis). These matrix elements contain information about how the energy levels vary as a function of X (see, for example, Pechukas 1983). We will use the notation $(d\hat{H}/dX)_{mn}$ to denote the matrix element $\langle\phi_m(X)|d\hat{H}/dX|\phi_n(X)\rangle$.

It is well known that random matrix models provide an excellent model for the short-ranged energy level statistics of almost all systems with a chaotic classical limit: some examples are given in a review by Berry (1983). There are three types of random

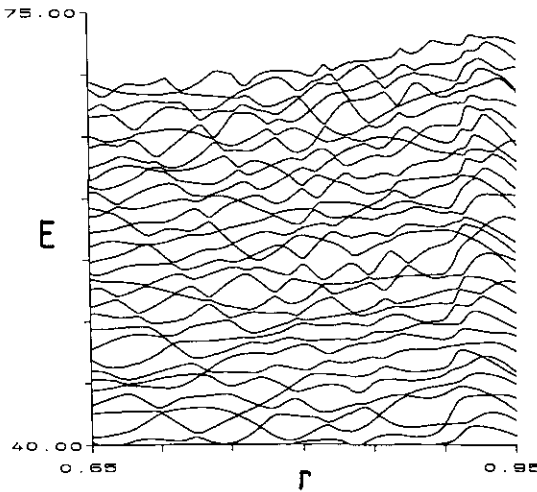


Figure 1. Energy levels of the modified Sinai billiard plotted for $40 \leq E \leq 80$; the levels are transformed to unit mean spacing. The highest level shown has quantum number $n = 70$.

matrix ensemble, the Gaussian orthogonal ensemble (GOE), Gaussian unitary ensemble (GUE), and Gaussian symplectic ensemble (GSE) (Porter 1965, Dyson 1962). The GOE is appropriate for systems with time-reversal symmetry and integral spin, the GUE applies to systems without time-reversal symmetry, and the GSE is applicable to systems with time-reversal symmetry and half integral spin. The elements of these random matrices are independent Gaussian random variables, with their variances chosen in such a way that the ensemble is invariant under the appropriate group of transformations (orthogonal, unitary or symplectic).

Much less is known about the statistical properties of the matrix elements. Using the suggestion of Berry (1977) that the wavefunctions of classically chaotic systems are quasi-random functions, it is possible to argue persuasively that the matrix elements we require are Gaussian distributed, and that the ratio of the variance of the diagonal matrix elements to those of the 'nearby' off-diagonal elements is the same as for the appropriate random matrix ensemble (Wilkinson 1990, appendix B). The off-diagonal elements have mean value zero, but the diagonal elements can have a non-zero mean. For example, if the system has GOE like energy-level statistics, it is expected that the variances of the matrix elements satisfy

$$\left\langle \left[\left\langle \left(\frac{d\hat{H}}{dX} \right)_{nm} \right\rangle - \left\langle \left(\frac{d\hat{H}}{dX} \right)_{nn} \right\rangle \right]^2 \right\rangle = 2 \left\langle \left(\frac{d\hat{H}}{dX} \right)_{nm}^2 \right\rangle \quad (1.1)$$

when m is close to (but not equal to) n , and the angle brackets indicate suitable averages over state labels n, m , which we discuss in section 3. In this paper we report numerical results on a particular example of a classically chaotic quantum billiard, which indicate that in the semiclassical limit the matrix elements are indeed Gaussian distributed, and satisfy (1.1). Alhassid and Feingold (1989) have also studied the statistical properties of the matrix elements of a classically chaotic system, and find that the transition strengths satisfy the Thomas–Porter (Porter 1965) distribution: this is equivalent to the matrix elements being Gaussian distributed.

A surprising finding from our work was that the semiclassical Gaussian distribution of the matrix elements only emerges slowly as the energy is increased, and we find that the distribution of matrix elements is much better described by the distribution

$$P_N(x) = \frac{\Gamma(N/2)}{\sqrt{\pi N} \Gamma\left(\frac{N-1}{2}\right)} \left(1 - \frac{x^2}{N}\right)^{(N-3)/2}. \quad (1.2)$$

This is the distribution of one component of an N -dimensional vector of length \sqrt{N} , uniformly distributed on the surface of an N -dimensional sphere (Porter and Rosenzweig 1960): it approaches a Gaussian in the limit $N \rightarrow \infty$. In appendix B we give tentative arguments which justify the use of this distribution for matrix element statistics of classically chaotic systems.

The GOE and other random matrix models can be extended to a family depending on a parameter X . By choosing an appropriate parametrization it is possible to ensure that both \hat{H} and $d\hat{H}/dX$ are elements of the random matrix ensemble (be it GOE, GUE or GSE), with the variance of the elements of both of these matrices independent of X . An example of such a parametrization is

$$\hat{H}(X) = \cos(X)\hat{H}_1 + \sin(X)\hat{H}_2. \quad (1.3)$$

Because of the invariance of these ensembles under the appropriate group of transformations, the statistics of the matrix elements of $d\hat{H}/dX$ remain unchanged when we transform to the eigenbasis of $\hat{H}(X)$. By allowing X to depend on time, it is also possible to model the dynamics of generic quantum systems under a time-dependent perturbation using (1.3) (Wilkinson and Austin 1992).

A parametrized GOE model was introduced in an earlier paper (Wilkinson 1989), where it was used to compute the density of avoided crossings. At that time it was not possible to test the application of the model to a chaotic quantum system, because of the large amount of data required to get good statistics. In this paper we illustrate the applicability of our model to a chaotic quantum billiard by calculating the density of avoided crossings and the probability distribution of second derivatives ('curvatures') of the energy levels with respect to a parameter. The distribution of the curvatures was originally calculated by Gaspard *et al* (1990) using a rather different approach to our own model. We re-derive their result using an expression for the density of avoided crossings, which was computed by Wilkinson (1989). Numerical studies of the curvature distribution for kicked quantum tops corresponding to the three types of matrix ensemble (Saher *et al* 1991), and for the stadium billiard (Takami and Hasagawa 1992), have confirmed the power law predicted theoretically. These studies did not consider the statistical properties of the matrix elements and were therefore unable to predict the numerical prefactors.

In section 2 we re-derive the distribution of large curvatures from the density of avoided crossings. Section 3 presents the results of a numerical study of a modified Sinai billiard, which validates the use of the parametrized GOE model: the statistical properties of the matrix elements are studied and the form of the curvature distribution and distribution of gap sizes are confirmed. The significant deviations of the matrix elements from the semiclassical limiting Gaussian form are discussed in appendix B.

2. Calculation of the curvature distribution

Gaspard *et al* (1990) have obtained expressions for the distribution of curvatures $K = (d^2E/dX^2)$ for a parameter dependent extension of the three matrix ensembles. Their method involves converting the parameter dependence of the energy levels into the equation of motion of an infinite gas of particles (Pechukas 1983); statistical mechanical arguments are used to obtain the tail of the distribution for large values of the curvature K . This quantity is related to the density of avoided crossings because large curvatures are correlated with the occurrence of avoided crossings. In this section we derive the distribution of large curvatures from the density of avoided crossings.

An avoided crossing in which a pair of levels approach to a separation which is much less than the mean level separation is characterized by three quantities, the gap size Δ , and the difference (A) and mean (B) of the two asymptotic slopes. The derivation of the density of avoided crossings (described in detail in Wilkinson (1989)) takes as a starting point a parametrized GOE Hamiltonian such as (1.3) with the variances of the matrix elements of \hat{H} and $d\hat{H}/dX$ independent of X . When two levels of such a system are close to an avoided crossing at parameter value X_0 , their behaviour can be parametrized using elementary degenerate perturbation theory as

$$E^\pm(X) = E_0 + B(X - X_0) \pm \frac{1}{2}[\Delta^2 + A^2(X - X_0)^2]^{1/2}. \quad (2.1)$$

In order to derive the density of avoided crossings from the form of expression (2.1) use is made of the statistics of the diagonal and near-diagonal elements of $d\hat{H}/dX$ in the basis formed by the eigenstates of $\hat{H}(X)$ (adiabatic basis); for a parametrized GOE the diagonal and off-diagonal matrix elements are Gaussian distributed with variances

$$\left\langle \left(\frac{d\hat{H}}{dX} \right)_{nm}^2 \right\rangle = (1 + \delta_{nm})\sigma^2 \quad (2.2)$$

(cf (1.1), but note that for the GOE both the diagonal and off-diagonal elements have zero mean). The statistical properties of the random variables E_0 , B , Δ , X_0 and A can be expressed in terms of those of the matrix elements of \hat{H} and $d\hat{H}/dX$. It is also necessary to make use of the form of the level spacing distribution for this system; for the GOE this has the form

$$P[S] dS = \frac{1}{6}\pi^2 n_0^2 S dS \quad (2.3)$$

for small S ; n_0 is the density of states (Porter 1965). Using the above information it is possible to obtain the density of avoided crossings as

$$N(A, B, \Delta) dA dB d\Delta = P[B] dB \frac{\pi n_0^2}{24\sigma^2} A^2 \exp(-A^2/8\sigma^2) dA d\Delta \quad (2.4)$$

where $P[B]$, the probability distribution of B , is a Gaussian with variance $2\sigma^2$. Full details of the calculation are given in Wilkinson (1989); the extension of the calculation to the GUE and GSE cases is straightforward. The results for the density of avoided crossings for the other ensembles are:

$$N(A, B, \Delta) dA dB d\Delta = P[B] dB \frac{\pi^{3/2} n_0^3 \Delta}{12\sigma^3} A^3 \exp(-A^2/4\sigma^2) dA d\Delta \quad (2.5)$$

for the GUE, with B Gaussian distributed with variance σ^2 and

$$N(A, B, \Delta) dA dB d\Delta = P[B] dB \frac{8\pi^{7/2} n_0^5 \Delta^3}{135\sqrt{2}\sigma^5} A^5 \exp(-A^2/2\sigma^2) dA d\Delta \quad (2.6)$$

for the GSE, with B Gaussian distributed with variance $\sigma^2/2$. In each case this density represents the density of avoided crossings with the relevant parameters encountered by a particular level with the level above it; including levels both above and below a given level introduces an additional factor of 2. It should be noted that the assumptions entering the derivation are minimal, i.e. statistics of the diagonal and next-to-diagonal matrix elements, and the level spacing distribution, so that only these minimal properties are needed to generalize the results to real systems.

The curvature distribution for the three ensembles can now be derived from the above results. Figure 2 is a schematic illustration of the variation of K as a function of the parameter X ; a maximum in K occurs at each avoided crossing. Define $dP = P[|K|] dK$ as the probability that the curvature satisfies $|K| \leq |d^2 E/dX^2| \leq |K| + d|K|$; from figure 2 this can be seen to be the sum of the absolute values of the projections on the X axis, each divided by the length of the interval ΔX :

$$dP = \frac{1}{\Delta X} \sum_i dP^{(i)}$$

$$dP^{(i)} = \left| \frac{dX}{dK} \right| dK. \quad (2.7)$$

In the vicinity of an avoided crossing expressions for K and dK/dX can be obtained from (2.1); since the position X_0 of the avoided crossing is irrelevant, we take $Y = (X - X_0)$ and obtain

$$\left| \frac{d^2 E}{dY^2} \right| = |K| = \frac{A^2 \Delta^2}{2(\Delta^2 + A^2 Y^2)^{3/2}} \quad (2.8)$$

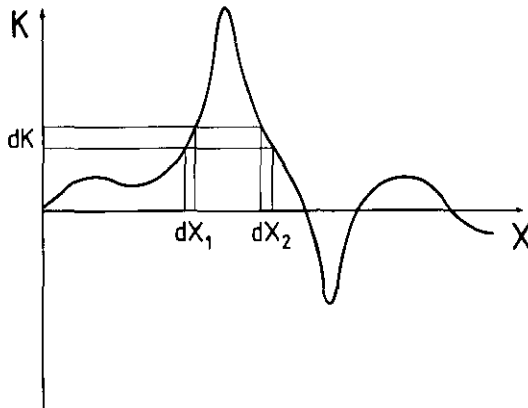


Figure 2. Schematic illustration of the variation of the curvature K of a level as a function of the parameter X . The curvature passes through a maximum at each avoided crossing. The contributions to $P(K)$ from one avoided crossing are indicated.

and

$$\left| \frac{d^3 E}{dY^3} \right| = \left| \frac{dK}{dY} \right| = \frac{3A^4 \Delta^2 |Y|}{2(\Delta^2 + A^2 Y^2)^{5/2}}. \tag{2.9}$$

Substituting for Y from (2.8), the derivative required in (2.7) is

$$\left| \frac{dY}{dK} \right| = \frac{2\gamma^{5/2} \Delta^{4/3}}{3A^3(\gamma \Delta^{4/3} - \Delta^2)^{1/2}} \tag{2.10}$$

with $\gamma = (A^2/2|K|)^{2/3}$.

As (2.10) is independent of B , $P[|K|]$ can be obtained as an integral over A and Δ ; this corresponds to estimating the sum in (2.7) by integrating over the density of avoided crossings.

$$P[|K|] = 4 \int_0^\infty dA \int_0^{A^2/2|K|} d\Delta f(\Delta, A) \left| \frac{dY}{dK} \right|(\Delta, A) \tag{2.11}$$

where f is obtained from the density of avoided crossings by integrating over B :

$$f(\Delta, A) = \frac{\pi n_0^2}{24\sigma^2} A^2 \exp(-A^2/8\sigma^2). \tag{2.12}$$

(For the GOE case f is independent of Δ ; we use this notation because the corresponding expressions for the GUE and GSE cases are functions of Δ as well as A .) The factor of four in (2.11) allows for the counting of avoided crossings due to levels both above and below a particular level and the double contribution (positive and negative values of dY/dK as shown in figure 2) for each avoided crossing. The expression (2.11) can be evaluated by first performing the integration with respect to Δ . This requires the evaluation of

$$I = \int_0^{\gamma^{3/2}} \frac{d\Delta \Delta^{4/3}}{(\gamma \Delta^{4/3} - \Delta^2)^{1/2}}. \tag{2.13}$$

The substitution $\Delta = \gamma^{3/2} \sin^3 \theta$ gives

$$I = 3\gamma^2 \int_0^{\pi/2} d\theta \sin^4 \theta = \frac{9\gamma^2 \pi}{16}. \tag{2.14}$$

Substituting this result into (2.11) gives

$$P[|K|] = \frac{\pi^2 n_0^2}{128\sigma^2 |K^3|} \int_0^\infty dA A^5 \exp(-A^2/8\sigma^2) \tag{2.15}$$

giving

$$P[|K|] = \frac{4\pi^2 n_0^2 \sigma^4}{|K^3|}. \tag{2.16}$$

Using the appropriate form of $f(\Delta, A)$ in (2.11) gives the form of $P[|K|]$ for the GUE and GSE:

$$P[|K|] = \frac{2^5 \pi^2 n_0^3 \sigma^6}{K^4} \tag{2.17}$$

and

$$P[|K|] = \frac{2^9 \pi^4 n_0^5 \sigma^{10}}{3K^6}. \quad (2.18)$$

Since these results are obtained using the density of avoided crossings with small energy gaps, they correspond to the large $|K|$ tail of $P[|K|]$; the small $|K|$ form of the curvature distribution cannot be obtained from this calculation. The results agree with those of Gaspard *et al*, confirming the correctness of both methods. In their calculations Gaspard *et al* use the parameter β , which is the inverse of the variance of dE/dX . β and σ are related by

$$\begin{aligned} \beta &= 1/2\sigma^2 & (\text{GOE}) \\ \beta &= 1/\sigma^2 & (\text{GUE}) \\ \beta &= 2/\sigma^2 & (\text{GSE}). \end{aligned} \quad (2.19)$$

For direct comparison their results must also be multiplied by 2 to convert from $P[K]$ to $P[|K|]$.

3. Numerical results for a parametrized billiard

In this section numerical results are presented on the matrix element statistics, number of avoided crossings as a function of gap size, and curvature distribution for a parametrized billiard model. The following results are obtained:

(i) The scaling properties of the matrix elements are obtained by considering the properties of the classical correlation function.

(ii) Using these scaling properties, the statistical properties of the matrix elements are shown to be in accordance with (1.1), i.e. the diagonal and off-diagonal elements are approximately Gaussian distributed with the variance of the diagonal elements twice that of the off-diagonal elements. The actual distribution of the matrix elements was in good agreement with (1.2), with the parameter N increasing in the semiclassical (large energy) limit.

(iii) Using an appropriate scaling, the expression (2.16) for the curvature distribution is shown to apply to this system, including the numerical factor. The number of avoided crossings with gap sizes between 0 and Δ is also obtained and shown to be in agreement with the theoretical expression derived from the density of avoided crossings (2.4) by integrating over all values of A and B and over energy gaps from zero to Δ .

The billiard model used is a variant of the Sinai billiard; the geometry is illustrated in figure 3. The variation of the eigenvalues as a function of the parameter r is shown in figure 1. The classical motion of this system is known to be purely chaotic with exponential divergence of all pairs of nearby orbits (Brown *et al* 1987). For the analysis of properties associated with avoided crossings, it is necessary to use a subset of states of one symmetry class. To obtain an appropriate subset of the eigenstates the numerical calculations were performed on the smaller domain (1/8 of the whole) shown by the bold line in the figure. The vanishing of the wavefunction on the perimeter of the small domain corresponds to a subset of states of one symmetry class for the entire billiard. The billiard differs from the usual Sinai billiard in having a concave boundary defined

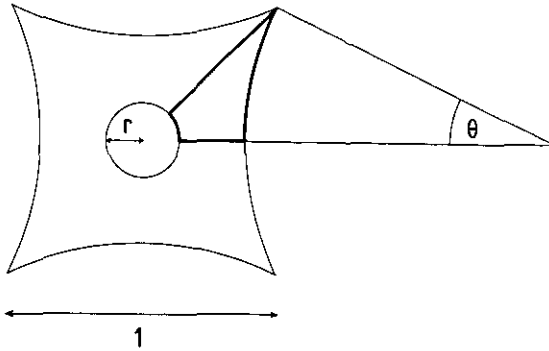


Figure 3. The modified Sinai billiard used in the numerical calculations.

by the angle θ ; this is introduced to eliminate the effect of a one-parameter family of unstable classical periodic orbits which can bounce between the straight sides of the usual Sinai billiard. Classical orbits of this type produce a slow ($1/t$) decay of the classical correlation function, which is undesirable for reasons which will be explained shortly.

The eigenvalues and matrix elements of $d\hat{H}/dr$ in the adiabatic basis were calculated for closely-spaced values ($\Delta r = 10^{-3}$) of the parameter r using the Green's function method described by Berry and Wilkinson (1984); the parameter θ was held constant at $\theta = 0.1$. A more detailed account of the calculation is given in appendix A. The set of energy levels obtained show the level repulsions expected for a classically chaotic system; it was verified that the level spacing distribution is of the form (2.3) for small values of Δ .

The matrix elements obtained have properties which differ from those of the matrix ensembles; whereas the latter are deliberately designed to have matrix elements with no dependence on energy, we anticipate the existence of energy-dependent structure in the statistical behaviour of the matrix elements of $d\hat{H}/dr$. This can be quantified by expressing statistical properties as a local function of energy. Denoting $d\hat{H}/dr$ by \hat{A} , the local second moment of the matrix elements is obtained as a function of the mean E and difference ΔE of the energies of pairs of states contributing to the sum.

$$\sigma^2(E, \Delta E) = \frac{1}{n_0^2} \sum_{n \neq m} \sum_m |\hat{A}_{nm}^2| \delta_\epsilon(E - \frac{1}{2}(E_n + E_m)) \delta_\epsilon(\Delta E - (E_n - E_m)). \quad (3.1)$$

Here the pseudo- δ functions are spread out over an energy range ϵ which is large compared to the mean level spacing but small compared to the classical energy scales of the problem. In the results presented below the technique of dividing each matrix element by the local standard deviation is used to obtain the underlying near-Gaussian distribution of the scaled matrix elements. This calculation is analogous to the procedure of accounting for the energy-dependence of the density of states when 'unfolding' a set of eigenvalues to unit mean spacing.

The variance of the off-diagonal elements can be related to the correlation function for the classical motion (Wilkinson 1987):

$$\sigma^2(E, \Delta E) = \frac{1}{2\pi\hbar\rho\Omega} \int_{-\infty}^{+\infty} dt C_A(E, t) \exp(i\Delta E t/\hbar) \quad (3.2)$$

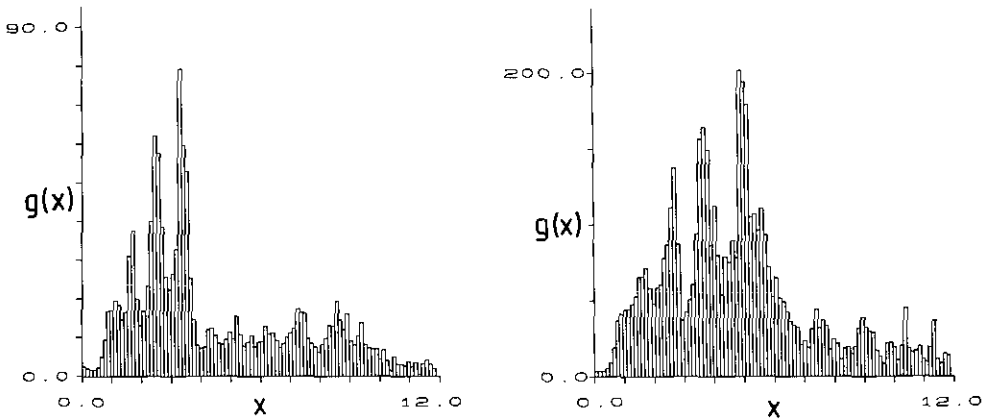


Figure 4. Plots of the function $g(x)$ ($x = \Delta E/\sqrt{E}$). The data were taken from matrix elements with r centred at (a) 0.72 and (b) 0.83.

where the correlation function $C_A(E, t)$ and the weight of the energy shell $\Omega(E)$ are defined as

$$C_A(E, t) = \int dq \int dp A(q, p) A(q'(q, p, t), p'(q, p, t)) \delta(E - H(q, p)) \quad (3.3)$$

(q', p') represents the phase space point that the point (q, p) evolves into after time t under the classical equations of motion) and

$$\Omega(E) = \int dq \int dp \delta(E - H(q, p)) \quad (3.4)$$

Unlike the stadium or the standard Sinai billiard, our system has a correlation function which decays faster than $1/t$, so that (3.2) converges. Because the classical trajectories of a particle in a billiard consist of free motion between reflections at the wall of the billiard, it can be seen that q and p can be expressed in terms of the energy E and scaled time variable $\tau = \sqrt{E}t$ as $q = Q(\tau)$, $p = \sqrt{E}Q'(\tau)$. Without considering the detailed form of the function Q and its derivative Q' (including the dependence on the initial coordinates and direction of the trajectory which has no effect on scaling properties), scaling arguments can be used to obtain the results that the correlation function is of the form $E^2 C_0(\sqrt{E}t)$ and that Ω is independent of E . These results allow a scaling relation for $\sigma^2(E, \Delta E)$ to be obtained:

$$\sigma^2(E, \Delta E) = E^{3/2} g\left(\Delta E/\sqrt{E}\right). \quad (3.5)$$

The function g is determined by the classical dynamics and hence depends on the value of the parameter r ; in the calculations described below the range $r = 0.65-0.95$ was processed in 12 subintervals such that $r \approx \text{constant}$ within each subinterval. This enabled the variation of g with r to be obtained. Since the calculation of the classical correlation function for this system presents considerable computational difficulties, we obtained the function $g(\Delta E/\sqrt{E})$ empirically. This was done by dividing each matrix element by $E^{3/4}$ and computing the variance of these scaled matrix elements as a function of the scaling variable $(\Delta E/\sqrt{E})$. The form of $g(\Delta E/\sqrt{E})$ is shown for two values of r in figure 4. We do not at present fully understand the complex structure of this function.

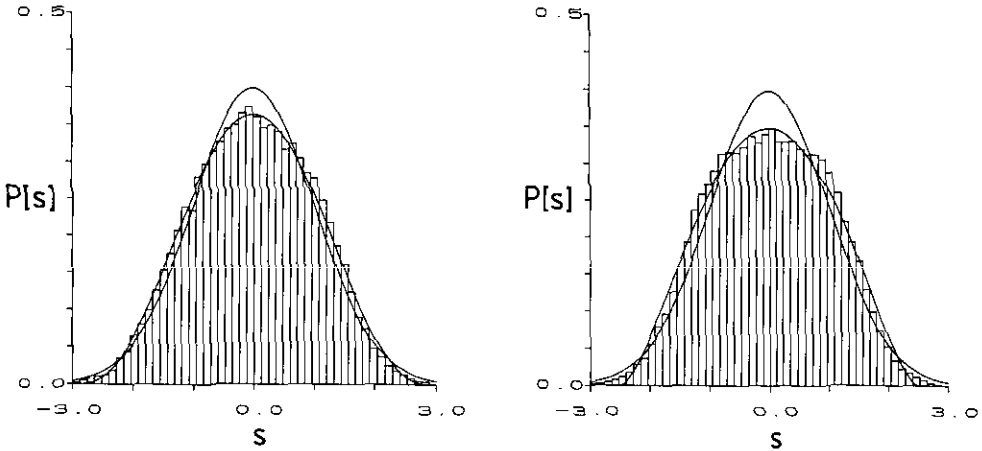


Figure 5. Distribution of scaled off-diagonal matrix elements s for all values of r : (a) $E \geq 65$, (b) $E \leq 40$. A Gaussian of unit variance and the best fit to the distribution (1.2) with (a) $N = 8.72$, (b) $N = 6.23$ are also shown.

The underlying form of the matrix element distribution was obtained by dividing each matrix element by the appropriate value of $\sigma(E, \Delta E)$ and combining the data for all r values; this would be expected to give a set of scaled matrix elements which are Gaussian distributed with zero mean and unit variance. The results, obtained using all matrix elements with $E \geq 65$, are illustrated in figure 5(a): they show a reasonable fit to a Gaussian, but they are fitted much more accurately by the distribution (1.2), with $N = 8.72$. The fit to a Gaussian is worse at lower energies: figure 5(b) shows results for all levels below $E = 40$, for which the best fit to (1.2) is $N = 6.23$. We discuss a possible reason why the distribution (1.2) fits that of the matrix elements in appendix B.

The variances of the scaled diagonal and near-diagonal $(n, n+1)$ and $(n, n+2)$ elements were calculated for $E \geq 65$, giving the result $1.86\sigma^2(E, \Delta E \approx 0) = \sigma_{\text{diag}}^2(E)$, reasonably close to the ratio of 2.0 predicted from (1.1). We assume that the deviation of the ratio of variances from 2.0 is due to the relatively poor statistics of the data. Although approximately 8000 near-diagonal and 4000 diagonal elements were available, data taken at adjacent r values are correlated, so the effective number of data points is much less than this. (The correlation length is given approximately by the mean distance between avoided crossings, which is large for low-lying states; even the highest states in figure 1 encounter only about 10–15 avoided crossings over the full range of r .)

The calculated billiard energy levels include about 200 avoided crossings with small gaps ($n_0\Delta \leq 0.5$). This number is insufficient for a full study of the avoided crossing density (2.4). It is however possible to study the partial statistic $F(\Delta)$ which is the number of avoided crossings with gap sizes between 0 and Δ . The theoretical expression (Wilkinson 1989) is

$$F(\Delta) = \int dr \int dE \frac{\pi}{3} \sqrt{\frac{\pi}{2}} n_0^2(r, E) \sigma_0(r, E) \Delta. \quad (3.6)$$

This expression is obtained from the density of avoided crossings (2.4) by integrating over all values of A and B and over energy gaps from zero to Δ . Here σ_0^2 is the variance of the near-diagonal elements of $d\hat{H}/dr$:

$$\sigma_0^2 = E^{3/2} g\left(\frac{\Delta E \approx 0}{\sqrt{E}}, r\right) = E^{3/2} f(r). \tag{3.7}$$

The function $f(r)$ was obtained numerically from a least squares fit to a linear function; the expression obtained was

$$f(r) = -3.25 + 7.13r. \tag{3.8}$$

(Use of a quadratic fit did not significantly affect any of the results discussed below.) The value of n_0 also varies with the billiard geometry and energy (Baltes and Hilf 1976):

$$n_0 = 1 - \frac{L}{2\sqrt{4\pi AE}} \tag{3.9}$$

where L is the length of the perimeter of the billiard and A is its area. The expression for $n_0^2\sigma$ was integrated over the range of r and E (r values from 0.66 to 0.92 and E values from zero to 85 were used). The gap sizes were obtained by identifying avoided crossings and fitting to (2.1) and the gaps were indexed in order of size. A plot of the total number of avoided crossings with gap sizes less than Δ should be a straight line with slope given by substituting (3.7),(3.8) and (3.9) into (3.6). This plot and the theoretical prediction are shown in figure 6 and can be seen to be in excellent agreement.

The curvature distribution was obtained from the full set of energy level data in a scaled form by calculating K numerically at each value of r and scaling each curvature:

$$K' = K/2\pi n_0 \sigma^2. \tag{3.10}$$

The large $|K'|$ tail of the scaled curvature distribution should, from (2.16), be

$$P(|K'|) dK' = |K'|^{-3} dK'. \tag{3.11}$$

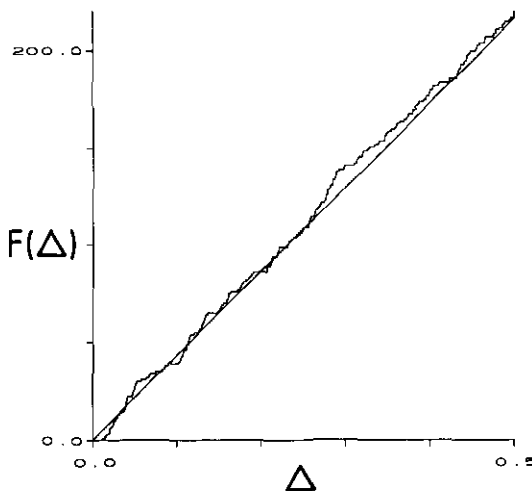


Figure 6. Plot of $F(\Delta)$ versus gap size for narrow avoided crossings. The theoretical expression (3.6) is also shown.

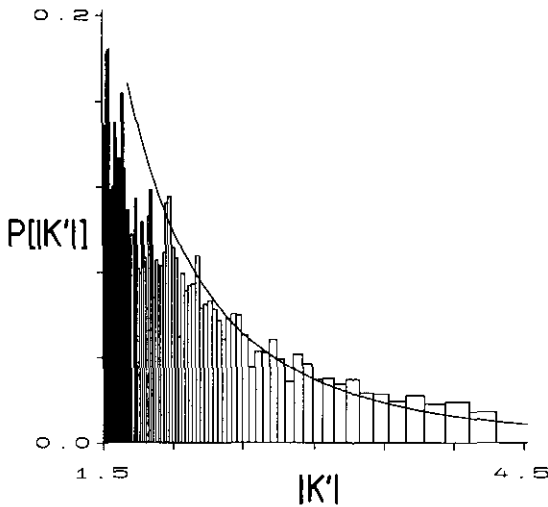


Figure 7. Histogram plot of the scaled curvature data; bins of width proportional to $|K'|^3$ are used so that each bin should contain the same number of points. The full line shows the theoretical curve (3.11).

This was confirmed by sorting the scaled curvatures into bins of width proportional to $|K'|^3$; figure 7 shows a histogram of the distribution of curvatures, compared with the theoretical prediction. It can be seen that both the $|K'|^{-3}$ form of the distribution and the prefactor (2.16) are correctly predicted. The fit of the large $|K'|$ tail is reasonable given the limited data, which only gives a small sample of large curvatures. Because a fixed value of Δr was used it was also necessary to reject a number of points with large values of $|K'|$, due to the breakdown of the finite-difference approximation to the derivatives.

4. Conclusion

In this paper we investigated the applicability of the parametrized GOE model to a chaotic quantum billiard and have verified that this random matrix model provides a good statistical description of the matrix elements of the quantum billiard. We have also shown that the parametrized GOE provides a good model for the density of avoided crossings, and the large $|K|$ tail of the curvature distribution.

We re-derived the theoretical form of the curvature distribution, originally obtained using the Pechukas level dynamics model, from the density of avoided crossings computed for the parametrized GOE. This result illustrates the close relationship between these two approaches.

We have found significant deviations of the distribution of matrix elements from the Gaussian form expected in the semiclassical limit. These deviations can be understood by noting that quite small numbers of matrix elements are constrained by the sum rule, (3.1) and (3.2).

Acknowledgments

The award of research grants by the Royal Society and the Science and Engineering Research Council are gratefully acknowledged.

Appendix A. Calculation of the eigenvalues and matrix elements of the billiard

The eigenfunctions of the billiard can be obtained by solving the Helmholtz equation

$$\nabla^2\psi + \frac{2mE}{\hbar^2}\psi = 0 \tag{A.1}$$

with $\psi(\mathbf{R}) = 0$ on the boundary of the billiard. We used units such that $\hbar = m = 1$. The energy levels were scaled to correspond to a system with area 4π , which gives a mean level density asymptotic to unity. Small deviations from this value are due to corrections related to the perimeter and curvature of the boundary and discontinuities at the corners (Baltes and Hilf 1976).

In order to compute the matrix elements it is necessary to specify exactly how the boundary is moved: it is not sufficient to specify how the shape varies; we must specify how the shape moves relative to a fixed coordinate frame. Although the diagonal matrix elements of the displacement are zero for displacements corresponding to translations or rotations of the boundary, the off-diagonal elements do not vanish. The matrix elements can be computed from the normal derivatives of the wavefunctions around the boundary and the displacement $\mathbf{d}(s) = d\mathbf{R}/dr$ of the boundary at arclength s due to the perturbation (Berry and Wilkinson 1984):

$$\langle \phi_n | \partial \hat{H} / \partial r | \phi_m \rangle = \oint ds \frac{\partial \psi_m}{\partial n}(s) \frac{\partial \psi_n}{\partial n}(s) \mathbf{d}(s) \cdot \hat{\mathbf{n}}(s). \tag{A.2}$$

We chose the displacement $\mathbf{d}(s)$ to be the sum of the displacement due to varying the radius r plus a multiple of \mathbf{R} corresponding to a uniform dilation of the system, with the origin at the centre of the interior scatterer of the billiard:

$$\mathbf{d}(s) = \chi(s)\hat{\mathbf{R}} + \mu\mathbf{R} \tag{A.3}$$

here $\chi(s)$ is unity if s lies on the curved segment parametrized by r and zero otherwise, and $\hat{\mathbf{R}}$ is the unit vector in the direction of \mathbf{R} . The value of μ was chosen so that the area of the billiard remains constant: we find

$$\mu = \frac{-\frac{\pi r}{4}}{\frac{\pi r^2}{4} + \frac{\theta}{\sin^2 \theta} - \frac{\cos \theta}{\sin \theta} - 1} \tag{A.4}$$

Appendix B. Distribution of matrix elements

Our results show that the distribution (1.2) is a good fit to the empirical probability distribution of matrix elements, normalized by dividing by the local value of their standard deviation. The distribution (1.2) is the distribution of one component of a random vector, uniformly distributed on the surface of an N -dimensional sphere of radius \sqrt{N} . This distribution was introduced by Porter and Rosenzweig (1960) in defining a random matrix ensemble similar to the GOE, in which the trace of the square of the matrix is rigidly constrained. The components of the eigenvectors of the GOE also clearly have the distribution (1.2). It is not however immediately clear why this distribution should characterize the matrix elements of a system with a classical limit. Here we present a tentative theory for this observation.

Equation (3.1) defines a sum rule which the matrix elements should satisfy, in the form of a constraint on the sum of the squares of the matrix elements in a range of energies of size ϵ : this is exactly the type of constraint which leads to the distribution (1.2). The sum is expressed in terms of classical quantities by means of (3.2): when ϵ is small, there are a series of corrections to (3.2) corresponding to the periodic classical orbits with periods up to $\tau = \hbar/\epsilon$ (Wilkinson 1987). This does not yet provide an explanation for the applicability of (1.2), because the number of matrix elements constrained by this sum,

$$N \approx \epsilon^2 n_0^2 \quad (\text{B.1})$$

can apparently be arbitrarily small. We must argue that the constraint imposed by the semiclassical sum rule expressed by (3.1), and (3.2) and its periodic orbit corrections, ceases to be valid if we make ϵ sufficiently small.

The periodic orbit corrections to (3.2) become meaningless for large values of the period τ , because they are based on semiclassical approximations which are not valid in the limit $\tau \rightarrow \infty$, with \hbar fixed (Wilkinson 1987). Because we consider a chaotic system, with exponentially diverging trajectories, the break time scales as

$$\tau^* \approx \tau_0 \log(S_0/\hbar) \quad (\text{B.2})$$

where τ_0 and S_0 are a characteristic time and action for the classical motion, which for a billiard scale as $E^{-1/2}$ and $E^{1/2}$ respectively. We assume that the sum rule ceases to constrain the matrix elements for values of ϵ smaller than \hbar/τ^* . Combining (B.1) and (B.2), we estimate that for a billiard system the leading order dependence of the parameter N on energy is

$$N \approx \text{const. } E/(\log E)^2 \quad (\text{B.3})$$

We have not been able to test this prediction, because for large N , the value of N fitted to the empirical data is very sensitive to statistical fluctuations in the data.

References

- Alhassid Y and Feingold M 1989 *Phys. Rev. A* **39** 374
 Baltes H P and Hilf E R 1976 *Spectra of Finite Systems* (B I Wissenschaftsverlag)
 Berry M V 1977 *J. Phys. A: Math. Gen.* **10** 2083
 — 1983 *Chaotic Behaviour of Deterministic Systems (Les Houches, Session XXXVI, 1981)* ed I Iooss, R H G Helleman and R Stora (Amsterdam: North-Holland)
 Berry M V and Wilkinson M 1984 *Proc. R. Soc. A* **392** 15
 Brown R, Ott E and Grebogi C 1987 *Phys. Rev. Lett.* **59** 1173
 Dyson F J 1962 *J. Math. Phys.* **3** 429
 Gaspard P, Rice S A, Mikeska H J and Nakamura K 1990 *Phys. Rev. A* **42** 4015
 Pechukas P 1983 *Phys. Rev. Lett.* **51** 943
 Porter C E (ed) 1965 *Statistical Properties of Spectra II: Fluctuations* (New York: Academic)
 Porter C E and Rozenzweig N 1960 *Ann. Acad. Sci. Fennicae A* **44** 4
 Saher D, Haake F and Gaspard P 1991 *Phys. Rev. A* **44** 7841
 Takami T and Hasegawa H 1992 *Phys. Rev. Lett.* **68** 419
 Wilkinson M 1987 *J. Phys. A: Math. Gen.* **20** 2415
 — 1989 *J. Phys. A: Math. Gen.* **22** 2795
 — 1990 *Phys. Rev. A* **41** 4645
 Wilkinson M and Austin E J 1992 *Phys. Rev. A* at press